Generation of Non-Rayleigh Speckle Distributions Using Marked Regularity Models

Robert M. Cramblitt, *Member, IEEE*, and Kevin J. Parker, *Fellow, IEEE*

Abstract—**Fully developed speckle patterns observed in coherent imagery are characterized by a Rayleigh-distributed envelope amplitude. Non-Rayleigh distributions are observed in many cases, such as when the number of scatterers in a resolution cell is small or scatterers are organized with some periodicity. Distributions resulting from the assumption of random scatterer phase (random walk models) have been used to describe the speckle amplitude in these cases, leading to K, Rician, and homodyned-K amplitude distributions. An alternative is to incorporate non-random phase implicitly by adopting models that directly describe the spatial placement of point scatterers. We examine the consequences of assuming that scattering is described in one dimension by a stationary renewal process in which the arrival times are the locations of ideal point scatterers, the interscatterer distances are drawn from a gamma distribution, and the scatterer amplitudes are allowed to be correlated in space. This model has been called the marked regularity model because variations of the model parameters can generate spatial distributions ranging from clustered to random to nearly periodic. We will demonstrate that all of the non-Rayleigh distributions generated by the previous random phase models can also be generated by the marked regularity model, and we show under what conditions the different distributions will result. We also demonstrate that the regularity model is inherently capable of describing certain sparse scattering conditions. Therefore, the model can represent many cases and provide an intuitively pleasing description of the spatial placement of the scatterers.**

I. Introduction

Speckle patterns are a characteristic feature of coherent imaging systems and are a consequence of the non-ideal nature of the system point-spread function. A large body of literature deals with the generation and statistical description of speckled images in optics, radar, and ultrasound. In systems that detect the echo or backscatter from a transmitted baseband signal modulated to frequency ω_0, the detected signal $r(t) = a(t)\cos(\omega_0 t + \phi(t)) = \Re\{a(t)e^{j\phi(t)}e^{j\omega_0 t}\}$, where $\Re\{\cdot\}$ denotes the real part, can be written as a complex phasor $\vec{A} = a(t)e^{j\phi(t)}$. If the imaging medium is modeled as a collection of small discrete scatterers, and the imaging system is assumed to be linear and space-invariant, the output $\vec{A}$ of a resolution cell can be viewed as the complex sum of contributions from each scatterer within the cell [1]:

$$\vec{A} = \frac{1}{\sqrt{N}} \sum_{1}^{N} a_n e^{j\phi_n}. \tag{1}$$

The mean power $E\{a_n^2\}$ reradiated by the discrete scatterer (such as a sufficiently small sphere) when multiple scattering is neglected (the Born approximation) is dependent on the size and type of the scatterer and the frequency of illumination [2], [3]. The phase ϕ_n depends on the position of the discrete scatterer with respect to the imaging system.

Attempts to model the statistical nature of speckle patterns typically fall into two broad categories: random walk models and spatial point process models. The former usually assumes that the positions of scatterers are random both within and between resolution cells. In specific cases, it is possible to derive the first-order probability density functions (PDF) of the amplitude (magnitude) of $\vec{A}$, but the resulting phase of $\vec{A}$ is random. For the spatial models, the phase of $\vec{A}$ depends on the assumed spatial structure; derivations of amplitude PDF become very difficult in this case.

We will demonstrate, via quantitative statistical analyses of random realizations of (1), that a single spatial point process model, referred to as the marked regularity model, is capable of producing amplitude PDF that are consistent with the random walk models and show how the regularity parameters affect the type of distribution generated. The marked regularity model provides a simple, intuitively pleasing description of the physical placement of point scatterers. It also allows the modeler to incorporate simple spatial amplitude correlations but provides closed-form descriptions of the power spectral density (PSD) of the process. The latter capability is important because second-order descriptions can provide a basis on which to differentiate between different backscatter signals when first-order statistics are essentially identical. In medical ultrasound, this provides a quantitative means of distinguishing between diseased and normal tissues.

Manuscript received May 6, 1998; accepted February 9, 1999. This work was supported by the Center for Electronic Imaging Systems and the University of Rochester Department of Electrical Engineering.

R. M. Cramblitt is with SVS Inc., Albuquerque, NM 87109-3425 (e-mail: robert.cramblitt@svsinc.com).

K. J. Parker is with the University of Rochester, Department of Electrical Engineering, Rochester, NY 14627-0231.

A. Random Walk Models

Random walk models assume that the phase associated with each scatterer in the resolution cell is random and independent of the amplitude; so (1) then represents a random walk in the complex plane. If the number of scatterers N in the resolution cell is very large or if the individual scatterer amplitudes a_n happen to themselves be Rayleigh-distributed, the resulting amplitude PDF is a Rayleigh density [1], [4]:

$$f_A(a) = \frac{2a}{\overline{a^2}} e^{-a/\overline{a^2}}, \tag{2}$$

which we refer to parametrically as the Rayleigh($\overline{a^2}$) PDF. This is the fully developed speckle case, also referred to as diffuse scattering.

If N is allowed to be random and happens to be drawn from the negative binomial distribution with parameter r, Jakeman [4] showed that the amplitude is then K-distributed whenever the mean number of scatterers $\overline{N}$ is sufficiently large, no matter what distribution a_n is drawn from:

$$f_A(a) = \frac{2b}{\Gamma(r)} \left(\frac{ab}{2}\right)^{Nr} K_{Nr-1}(ba) \tag{3}$$

where $b = 2\sqrt{r/\overline{a^2}}$, which we refer to as the K($r, \overline{a^2}, N = 1$) PDF. If the individual scatterer amplitudes a_n happen to be K-distributed, Jakemen showed that the amplitude PDF would be K($r, \overline{a^2}, N$), no matter what N happens to be. When the parameter r is very large, the amplitude becomes Rayleigh-distributed, but smaller values of r are associated with the clustering of scatterers. Oliver [5] developed the second-order properties of speckle intensity in the K-distributed case for certain scatterer amplitude distributions and correlations.

Fig. 1 provides examples of different random-walk-based distributions. As Fig. 1 demonstrates, the peak of the K density is shifted toward the origin, and the area under the tail is greater than that of the Rayleigh density. The difference between the two densities is manifested as a subtle shift in the tails of the PDF when r is of intermediate magnitude.

A nonrandom term S representing a specular or unresolved coherent component can be added to (1); under the same assumptions as in the Rayleigh case, the amplitude PDF is a Rician density [1], [2]:

$$f_A(a) = \frac{2a}{\overline{a^2}} I_0\left(\frac{2aS}{\overline{a^2}}\right) e^{-(a^2+S^2)/\overline{a^2}}, \tag{4}$$

which we refer to as the Rice($S, \overline{a^2}$) PDF. Such a component might arise when scatterers occur at quasi-periodic intervals that are so short that the first harmonic peak induced in the RF spectrum by the periodicity occurs above the system bandpass. Wagner *et al.* [2] allowed S to vary spatially in a deterministic fashion, making (4) into a generalized Rician density, and examined the second-order statistics of speckle intensity. In particular, S was allowed to represent a nonrandom periodic spatial variation.

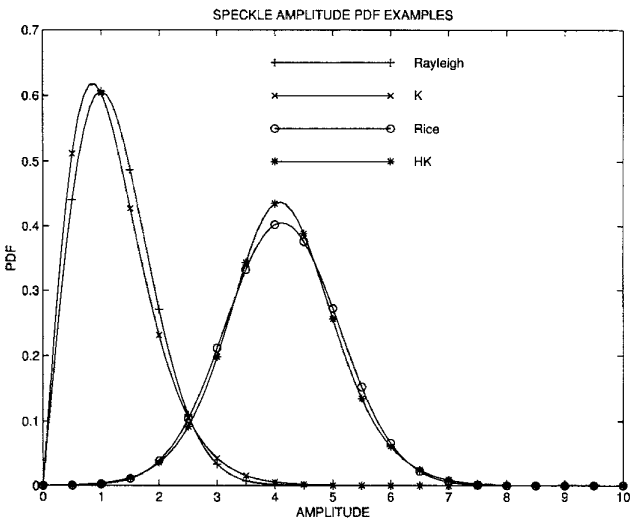

Fig. 1. Examples of the Rayleigh, K, Rice, and homodyned-K density functions.

As in the Rician case, a nonrandom specular term may be added to (1), while maintaining the assumptions required for the development of the K distribution. In this case, the resulting amplitude PDF is a homodyned-K density [6]:

$$f_A(a) = a \int_0^\infty \frac{uJ_0(uS)J_0(ua)}{(1 + u^2\overline{a^2}/4r)^r} du \tag{5}$$

for which no closed form solution exists and which we refer to as the HK($r, S, \overline{a^2}$) PDF.

The homodyned-K density differs from the Rician density in much the same way as the K-density differs from the Rayleigh, as Fig. 1 illustrates.

Jakeman and Tough [7], [8] described the relationships among all of the previously mentioned random walk models and proposed a generalized K distribution that can simplify to K or Rician distributions under the appropriate conditions, although they point out that there are certain difficulties with this approach. Their approach does include some limited departures from the assumption of random scatterer phase, as does the approach of Barakat [9]. If the number of scatterers in the random walk is very small, Daba and Bell [10] showed that solutions could be derived for the intensity (squared-amplitude) PDF.

Various researchers have proposed applying random walk models to the analysis of medical ultrasound data. In addition to the already cited work of Wagner *et al.* [2] and Dutt and Greenleaf [6], Shankar [11] adapted Jakeman's derivations for the ultrasound context, and Molthen *et al.* [12] and Narayanan *et al.* [13] proposed using estimates of the parameters of the K distribution in combination with other measures to characterize tissue measurements.

B. Spatial Models

Spatial models attempt to describe the physical placement of point scatterers and can, therefore, describe cases in which the phase of each scatterer is not uniformly distributed. The simplest spatial model treats scatterers as the points of a Poisson point process. This is equivalent to the random walk model in that scatterers appear to be placed completely at random. Tuthill *et al.* [14] suggested using a combination of a Poisson point process and a perfectly periodic process to model ultrasonic scattering from tissues that have some regularly spaced structures. They showed that amplitude PDF corresponding to Rayleigh, Rician, and what they termed pre-Rayleigh could develop as the density of scatterers decreased. The regularity model was proposed by Landini and Verrazzani [15] to describe both random and regular (but not perfectly regular) spatial placements. This model treats scatterers as points of a stationary renewal process, of which the Poisson process is a special case. Cramblitt and Bell [16] investigated the estimation of regularity model parameters based on sparse spectral estimates and extended the model to allow for nonuniform scatterer amplitudes (marks) [17]. It is this model that we will consider in depth subsequently. Landini *et al.* [18] demonstrated that the regularity model would predict pre-Rayleigh amplitude PDF at low scatterer concentrations.

Varghese *et al.* [19], [20] employed a model similar to the regularity model to show that spectral autocorrelation functions could detect quasi-periodic scatterer placements. Weng *et al.* [21], [22] used simulations from another quite similar model to show that certain types of phase nonuniformities develop at various frequencies in the presence of quasi-periodic spatial placement. They proposed several measures to detect these nonuniformities. Ohya *et al.* [23] used a jittered-lattice model to demonstrate that the amplitude signal-to-noise ratio would be enhanced in the presence of quasi-periodic scattering. The jittered-lattice model assumes that all scatterers occur at locations that are randomly offset from a fixed periodic lattice; the offsets are small with respect to the period. This type of model was also used by Narayanan *et al.* [24] in an investigation of methods to detect phase nonuniformity caused by quasi-periodic scattering.

Shankar *et al.* [25], combining aspects of both random walk and spatial models, used parameters of the K distribution as well as a χ^2 test of phase nonuniformity in an attempt to detect lesions of the breast. Abeyratne *et al.* [26] proposed using a superposition of marked regularity models to model tissue structure and proposed the characterization of tissues based on third-order statistical properties, although their theoretical development was limited to a combination of random and perfectly periodic scattering processes.

In this paper, we build on the links that have been established between quasi-periodic scattering and non-Rayleigh PDF, showing that all of the common non-Rayleigh densities can be generated by adjusting the parameters of the marked regularity model. Although most attention has been focused on the ability of this model to describe quasi-periodic structure, it also describes the clustering of scatterers, which is significant because clustering is the underlying premise of the random walk model leading to K distributions. We will begin by reviewing the description of the marked regularity model and then use computer simulations to investigate the first-order distributions generated by this model.

II. Marked Regularity Models

The regularity model treats scatterers as the points of a stationary renewal point process in which the distances between points are gamma-distributed. This process is described by the scatterer function,

$$s(t) = \sum_i m_i \delta(t - T_i), \tag{6}$$

in which the $\{T_i\}$ are an ordered sequence of scatterer locations expressed as temporal delay times. This function can be viewed as the time domain equivalent of (1). The $\{T_i\}$, defined so that $T_0 \leq 0 \leq T_1$, are then the recurrence times from the origin of the renewal process. The marks correspond to the $\{a_n\}$ of (1) and represent the detected amplitudes of the wave reflected by the scatterers. We assume that the interscatterer times $\{x_i\}$ are independent, identically distributed (i.i.d.) random variables from a gamma(α,β) distribution, which has a density function:

$$f(x) = \frac{x^{\alpha-1}e^{-x/\beta}}{\Gamma(\alpha)\beta^\alpha} \quad \alpha, \beta, x > 0 \tag{7}$$

where $\Gamma(\alpha)$ is the gamma function:

$$\Gamma(\alpha) = \int_0^\infty t^{\alpha-1}e^{-t}dt. \tag{8}$$

This density, unlike a Gaussian, for example, is consistent with the assumptions underlying the existence of a stationary random process [27]. The mean and variance of the interscatterer times are $\overline{x} = \alpha\beta$ and $\sigma_x^2 = \alpha\beta^2 = \overline{x}^2/\alpha$, respectively. Thus, for a given mean interscatterer spacing, $\overline{x}$, the variance of the interscatterer times is controlled by varying the model order α. If α is large, the variance of the interscatterer times becomes small, and the scatterers become very regularly spaced. In the limiting case, the scatterers have a periodic spacing. If $\alpha = 1$, the $\{x_i\}$ are exponentially distributed, and the model reduces to a Poisson point process. In this case, the scatterers appear to have a random placement, and the degree of regularity is considered small. Values of α less than unity cause the scatterers to appear clustered. Fig. 2 demonstrates this behavior for various values of α when the mean interscatterer distance is maintained at unity. Notice that the spatial organization differs remarkably even though the mean

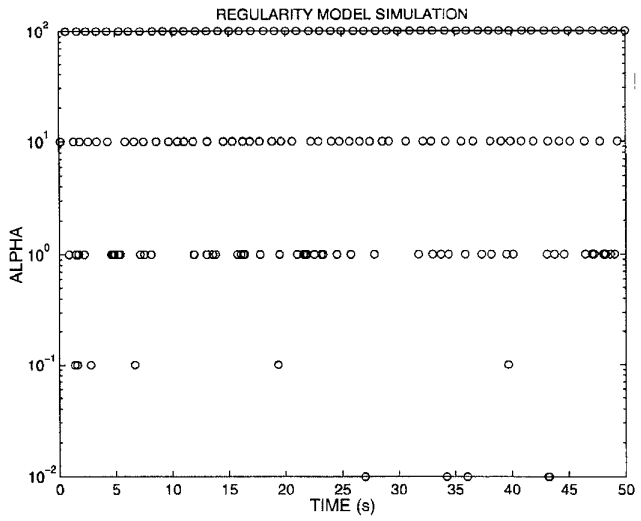

Fig. 2. Demonstration of spatial scatterer organization as the regularity model order is varied while $\overline{x}$ is held at a constant value of 1 scatterer/s. Each circle represents the location of a scatterer, except in the $\alpha = 0.01$ case, where each represents a cluster of scatterers falling too close together to resolve on this scale.

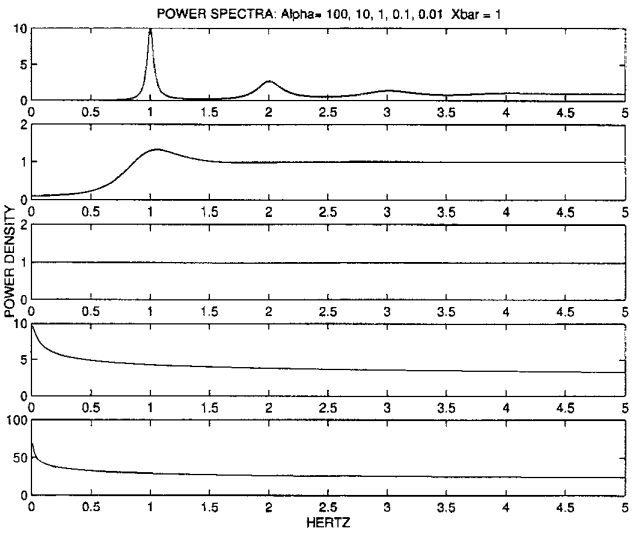

Fig. 3. Power spectra of processes corresponding to those shown in Fig. 2. From top to bottom, $\alpha = 100, 10, 1, 0.1, 0.01$.

interscatterer distance is the same in each case. Note that it is possible to maintain a minimum scatterer spacing by adding a shift to the interscatterer density function.

The straightforward description of the physical placement of scatterers is one of the key features of the regularity model. The other is that second-order statistical descriptions of the process are known. The PSD of the unmarked ($m_i = 1$) scatterer function is:

$$\Phi_s(\omega) = \frac{1}{\overline{x}} \left[\frac{|Z|^2 - 1}{|Z - 1|^2} \right], \quad \omega \neq 0, \tag{9}$$

where

$$Z = (1 - j\omega\overline{x}/\alpha)^{\alpha}. \tag{10}$$

This PSD is constant for $\alpha = 1$ and develops peaks near the harmonics of $1/\overline{x}$ (Hz) as α increases. At large frequencies, it becomes equal to $1/\overline{x}$. If $\alpha < 1$, the PSD decreases monotonically from the origin. Fig. 3 shows the power spectra of the processes corresponding to those shown in Fig. 2. The mean power spectrum of a finite interval (e.g., a resolution cell) of the regularity process can be approximated in closed form as long as the mean number of scatterers in the interval is sufficiently large [16].

For certain cases of mark correlation functions, the PSD of the marked regularity process may be written in either open or closed forms, depending on the mark correlation being a function of time (temporal correlation) or location in the arrival time sequence (sequential correlation). Closed form approximations of the mean power spectrum of finite intervals exist in either case [17]. The existence of PSD expressions allows long-range correlation of scatterer amplitude to be incorporated into the scattering model so that, for example, the random spatial behavior of the Poisson point process case ("diffuse scattering") can be combined with a damped-sinusoidal mark correlation to incorporate quasi-periodic variations in a simple manner.

In the next section, we describe the results of simulations designed to examine the first-order statistics that result from the assumption of the basic regularity model.

III. Simulations

We simulated the scattering function modeled by the regularity process and convolved it with a gated cosine pulse to simulate a detected RF signal. A gated cosine pulse of length T was chosen so that only scatterers within the well-defined distance of $\pm T/2$ could affect the RF signal at any point. A Gaussian pulse envelope can be used, but the effective number of interfering scatterers is not as precisely defined. The period of the cosine was 10 samples, one RF sample was obtained at the center of every resolution cell, and 1000 sequential resolution cells were sampled. We used uncorrelated log-normal marks with mean $\overline{m} = 1$ and variance $\sigma_m^2 = 0.1$. Simulations were carried out for various combinations of α, T, and $\overline{x}$. T was chosen so that the mean number of scatterers per resolution cell, $T/\overline{x}$, varied logarithmically from 2 to 50. $\overline{x}$ was chosen to be either 2.5 or 3 periods of the cosine used in the RF pulse, and α was varied logarithmically from 0.03 to 100. The two choices for $\overline{x}$ were motivated by the fact that scatterers should produce constructive interference when periodically spaced at even multiples of quarter wavelengths and should produce destructive interference when spaced at odd multiples of a quarter wave.

The simulation was repeated five times, and the collection of RF samples was used to form a histogram estimate of the PDF and integrated to estimate the cumulative distribution function (CDF). We compared the observed

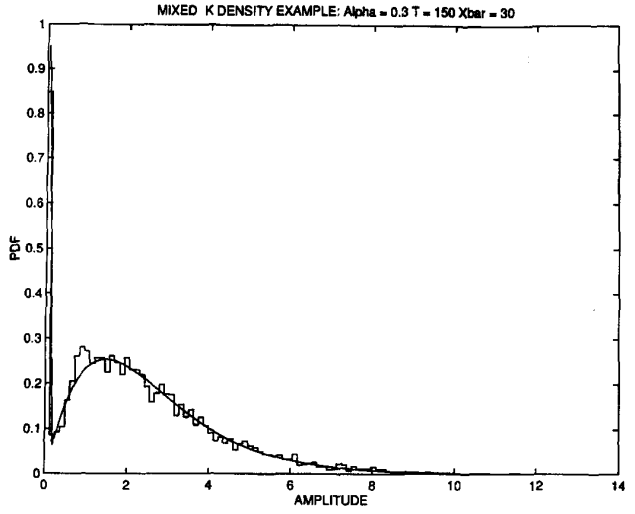

Fig. 4. Example of the mixed behavior that develops as either α or the mean number of scatterers per cell decreases. The smooth line is the parametric mixed K density best fitting the data (stepped line).

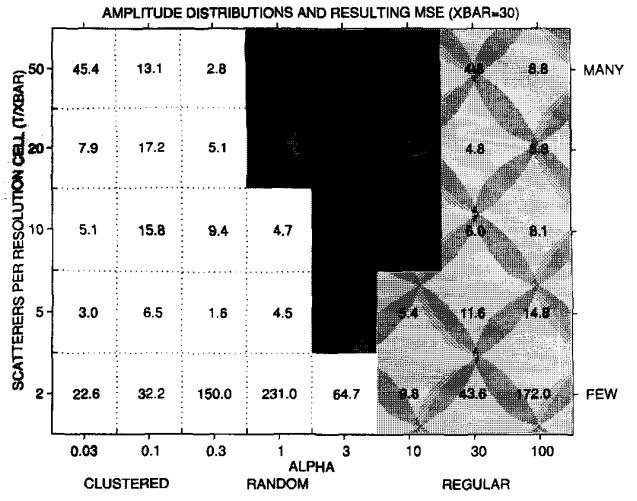

Fig. 5. Chart showing which of the Rayleigh, Rician, or K distributions best fit the CDF simulated for the values of α and $T/\overline{x}$ shown. $\overline{x}$ = three cycles of the RF pulse. Numbers indicate the MSE of the comparison. Boxes with the darkest shading indicate that the Rayleigh CDF fit best, medium shading indicates that the Rician CDF fit best, and no shading indicates that the K CDF fit best.

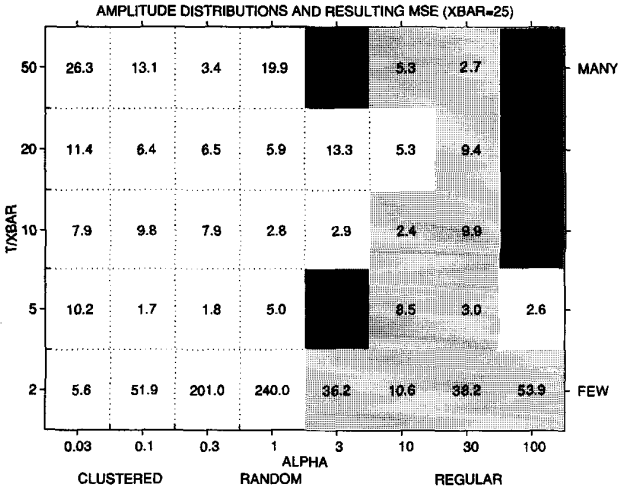

Fig. 6. Chart showing which of the Rayleigh, Rician, or K distributions best fit the CDF simulated for the values of α and $T/\overline{x}$ shown. $\overline{x} = 2.5$ cycles of the RF pulse.

CDF to that of the Rayleigh, Rician, and K distributions by computing a mean-squared error (MSE). The Rayleigh CDF used was that with the same mean-squared value as the data, which is a maximum likelihood (ML) estimate. The parameters of the Rician were also ML estimates, although a simple optimization is required to find them. Because no closed-form ML solution for the K distribution exists, we set its mean-squared value equal to the sample mean square and found the r parameter by minimizing the MSE between the K and the observed distribution. The distribution with the lowest MSE is considered to have the best fit to the data among the three distributions, even though the best fit may be rather poor, as we shall see.

IV. Results

A limitation of most random walk-based models is that they assume that resolution cells contain large numbers of scatterers so that there is little chance that the resolution cell contains no scatterers; hence, the PDF have zero value at the origin. However, when the number of scatterers per resolution cell is small or when significant clustering of scatterers occurs, the probability that zero scatterers fall in a resolution cell becomes significant. We observed this behavior manifesting itself as a peak in the PDF at the origin as scatterers became more clustered (small α) or as their concentration decreased (small $T/\overline{x}$). Fig. 4 illustrates this behavior. In this case, a density that would otherwise seem to be well modeled by a K density contains a peak near the origin. We found that such cases could be modeled by using a mixture of a K density and a discrete density consisting of a single delta function at the origin with a magnitude equal to the probability that zero scatterers fall in a resolution cell, $\Pr(N_T = 0)$, which can be calculated from the parameters of the regularity model. The data provided by Landini *et al.* [18] provides experimental confirmation of this behavior, which, in their case, developed as the mean scatterer concentration of a phantom was decreased. We included the mixed term when comparing the simulated PDF to K densities.

From the three theoretical CDF under consideration, we determined the one best fitting the observed CDF in the mean-squared sense and present this information in Figs. 5 and 6.

The HK PDF combines features of the Rice and K PDF; therefore, it is natural to speculate that it arises as the result of a combination of periodic structure and clustering.

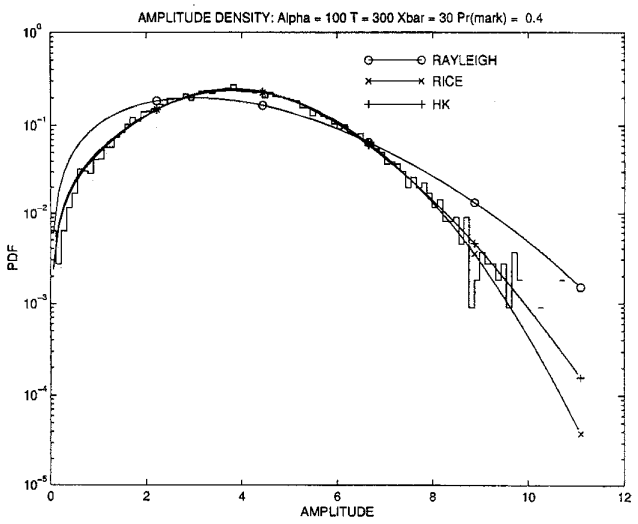

Fig. 7. Example of data for which a homodyned-K PDF appears to provide a better fit than a Rician or Rayleigh PDF. A logarithmic scale helps to visualize the difference between the Rician and homodyned-K curves.

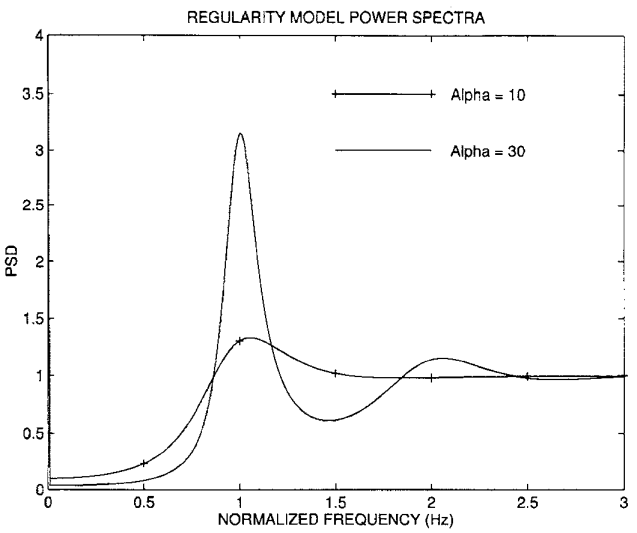

Fig. 8. Power spectral densities of the regularity process for cases $\alpha = 10$ and 30 and $\overline{x} = 1$. The $\alpha = 30$ case displays multiple spectral peaks.

We tried to generate such a case by taking a simulation from a case seen to result in Rician statistics and randomly extinguishing marks with a probability of 0.6. This reduces their frequency of occurrence and maintains the quasi-periodic spacing expected of a large α case. Fig. 7 shows the result of this sparse scattering experiment along with the Rayleigh, Rician, and HK densities best fitting the data. The MSE of the HK PDF shown is 9.2 versus 18.0 for the Rician PDF. The first three relative intensity moments (often used to solve for PDF parameters), $\overline{a^{2n}}/(\overline{a^2})^n$, $n = \{2, 3, 4\}$, were 1.6, 3.4, and 9.1 for the observed data; 1.6, 3.2, and 8.2 for the Rician PDF; and 1.6, 3.4, and 9.3 for the HK PDF.

V. Discussion

Regularity models in which $\alpha = 1$ represent Poisson point processes corresponding to the random walk; therefore, we expect that as the number of scatterers per resolution cell becomes large, Rayleigh amplitude statistics will develop. This was observed, although Rayleigh behavior is not quite developed at 10 scatterers per cell, which is often taken to be the point at which fully developed speckle is present. Larger values of α correspond to quasi-periodic scatterer placement; the cases in Fig. 5 correspond to placement at a spacing that should result in constructive interference of RF pulses; the cases in Fig. 6 should result in destructive interference.

Rician statistics were observed to result at the largest values of α in the constructive interference cases; the same cases revert to K or Rayleigh behavior in the destructive interference cases. This is in agreement with the simulations performed by Tuthill *et al.* [14] and is explained by viewing the effect of destructive interference as a phenomenon that reduces the effective number of contributing scatterers, resulting in K distributions or possibly Rayleigh distributions if there are a sufficient number of effective scatterers.

Cases in which the scatterer density is small (small $T/\overline{x}$) or cases in which clustering becomes important are best described by the K distribution. This agrees with the observation of pre-Rayleigh densities in [14] and [18].

Of course, there is no requirement or expectation that the distributions generated by the regularity model should be limited to the three special cases that we have considered. In fact, examination of the MSE in each of the charts reveals various regions in the parameter space for which the error is quite large, implying that none of the three PDF is an appropriate model. Consider, for example, cases in which α is extremely large, so that the resulting scatterers exhibit only slight deviations from perfect periodicity (the jittered-lattice model referred to earlier). The resulting amplitude distributions should then become essentially Gaussian-type PDF with the mean equal to $\overline{m}T/\overline{x}$. Values of α lying between these and those giving Rician statistics will result in an intermediate type of PDF that is difficult to describe with any simple, well-known parametric PDF. Interested readers may wish to consult Daba and Bell's work [10] describing intensity PDF for small numbers of randomly placed scatterers.

The existence of a PSD formula for the marked regularity process may be especially useful when trying to develop tests to distinguish between RF signals arising from scattering distributions whose first-order statistics are quite similar. For example, the two Rician cases of Fig. 5, corresponding to $T/\overline{x} = 5$ and $\alpha = 10$ and 30, have almost identical Rician parameters ($S = 1.3$, $\overline{a^2} = 4$), but the PSD of the two underlying regularity processes differ considerably as is illustrated in Fig. 8. The work by Cramblitt and Bell

[16], [17] examined the feasibility of estimating regularity model parameters from sparse samples of the power spectrum. The use of spectral autocorrelation functions [19], [20] and third-order statistics [26] is also of considerable interest and should be explored within the context of the marked regularity model.

No attempt was made here to assess how many RF samples are required to exploit the properties of the marked regularity model. This is a critical issue in attempting to perform tissue characterization in medical ultrasound because uniform regions of tissue can be quite small. Separate investigations are required to address this issue. This does not preclude the use of the model to generate synthetic scenes with amplitude distributions of interest, however, or to assist in the statistical analysis of such scenes. We have also made no attempt to model mark correlations or to relate the model to scattering from particular types of tissue; these items fall under the scope of future work. Various efforts have been made to study tissue scattering in the context of the random walk and spatial models described earlier, and new first principle models for tissue scattering [28] hold the potential to provide a means of validating these statistical approaches. We have cited instances in which experimental evidence exists to confirm some of our observations, but additional experimental work, particularly with well-controlled phantoms, would be of considerable interest.

VI. Conclusions

We have demonstrated through the use of computer simulations that the marked regularity model is capable of generating scatterer processes that result in the RF amplitude distributions that have been most frequently analyzed in the literature and for which there is ample experimental evidence. Adjustment of the basic regularity parameters allows random, clustered, and quasi-periodic structure to be generated within a single model, and Rayleigh, Rician, K, and homodyned-K distributions are generated, depending on the mean interscatter distance and RF center frequency, the regularity model order, and the number of scatterers per resolution cell. The model's simple description of scatterer placement in terms of random interscatterer distances is intuitively pleasing, and the existence of formulas for the PSD is potentially of great use in discriminating between cases exhibiting similar first-order statistics. The ability to incorporate spatial correlations is particularly promising as a stochastic means of describing long range structure. Unlike certain results based on random-walk-based speckle models for large numbers of scatterers, the regularity model is not limited to cases in which the mean number of scatterers is large and can, therefore, predict enhancement of the PDF near the origin at low scatterer densities.

References

[1] J. W. Goodman, "Statistical properties of laser speckle patterns," in *Laser Speckle and Related Phenomenon*, 2d. ed. J. C. Dainty, Ed., New York, NY: Springer-Verlag, 1984, ch. 2.

[2] R. F. Wagner, M. F. Insana, and D. G. Brown, "Statistical properties of radio-frequency and envelope-detected signals with applications to medical ultrasound," *J. Opt. Soc. Amer. A, Opt. Image Sci.*, vol. 4, no. 5, pp. 910–922, May 1987.

[3] A. D. Pierce, *Acoustics: An Introduction to its Physical Principles and Applications*. New York, NY: Acoust. Soc. Amer., 1989.

[4] E. Jakeman, "On the statistics of K-distributed noise," *J. Phys. A, Math. Gen.*, vol. 13, no. 1, pp. 31–48, Jan. 1980.

[5] C. J. Oliver, "A model for non-Rayleigh scattering statistics," *Optica Acta*, vol. 31, no. 6, pp. 701–722, Jun. 1984.

[6] V. Dutt and J. F. Greenleaf, "Ultrasound echo envelope analysis using a homodyned K distribution signal model," *Ultrason. Imaging*, vol. 16, no. 4, pp. 265–287, Oct. 1994.

[7] E. Jakeman and R.J.A. Tough, "Generalized K distribution: A statistical model for weak scattering," *J. Opt. Soc. Amer.*, vol. 4, no. 9, pp. 1764–1772, Sept. 1987.

[8] ——, "Non-Gaussian models for the statistics of scattered waves," *Adv. Phys.*, vol. 37, no. 5, pp. 471–529, 1988.

[9] R. Barakat, "Weak-scatterer generalization of the K-density function with application to laser scattering in atmospheric turbulence," *J. Opt. Soc. Amer. A, Opt. Image Sci.*, vol. 3, no. 4, pp. 401–409, Apr. 1986.

[10] J. S. Daba and M. R. Bell, "Statistics of the scattering cross-section of a small number of random scatterers," *IEEE Trans. Antennas Propagat.*, vol. 43, no. 8, pp. 773–783, Aug. 1995.

[11] P. M. Shankar, "A model for ultrasonic scattering based on the K distribution," *Phys. Med. Biol.*, vol. 40, no. 10, pp. 1633–1649, Oct. 1995.

[12] R. C. Molthen, P. M. Shankar, and J. M. Reid, "Characterization of ultrasonic B-scans using non-Rayleigh statistics," *Ultrason. Med. Biol.*, vol. 21, no. 2, pp. 161–170, 1995.

[13] V. M. Narayanan, P. M. Shankar, and J. M. Reid, "Non-Rayleigh statistics of ultrasonic backscattered signals," *IEEE Trans. Ultrason., Ferroelect., Freq. Contr.*, vol. 41, no. 6, pp. 845–851, Nov. 1994.

[14] T. A. Tuthill, R. H. Sperry, and K. J. Parker, "Deviations from Rayleigh statistics in ultrasonic speckle," *Ultrason. Imaging*, vol. 10, no. 2, pp. 81–89, 1988.

[15] L. Landini and L. Verrazzani, "Spectral characterization of tissues microstructure by ultrasounds: A stochastic approach," *IEEE Trans. Ultrason., Ferroelect., Freq. Contr.*, vol. 37, no. 5, pp. 448–455, Sep. 1990.

[16] R. M. Cramblitt and M. R. Bell, "Surface characterization using frequency diverse scattering measurements and regularity models," *IEEE Trans. Signal Processing*, vol. 44, no. 3, pp. 599–610, Mar. 1996.

[17] ——, "Marked regularity models," *IEEE Trans. Ultrason., Ferroelect., Freq. Contr.*, vol. 46, no. 1, pp. 24–34, Jan. 1999.

[18] L. Landini, M. F. Santarelli, and L. Verrazzani, "Microstructural properties reflected on the envelope and power spectral density of the RF image from tissue-like phantoms," in *Signal Processing V: Theories and Applications: Proc. EUSIPCO-90, 5th Eur. Sig. Proc. Conf.*, vol. 2, Barcelona, Spain, 1990, pp. 935–938.

[19] T. Varghese and K. D. Donohue, "Characterization of tissue microstructure scatterer distribution with spectral correlation," *Ultrason. Imaging*, vol. 15, no. 3, pp. 238–254, Jul. 1993.

[20] K. D. Donohue, J. M. Bressler, T. Varghese, and N. M. Bilgutay, "Spectral correlation in ultrasonic pulse echo signal processing," *IEEE Trans. Ultrason., Ferroelect., Freq. Contr.*, vol. 40, no. 4, pp. 330–337, Jul. 1993.

[21] L. Weng, J. M. Reid, P. M. Shankar, K. Soetanto, and X.-M. Lu, "Nonuniform phase distribution in ultrasound speckle analysis—Part I: Background and experimental demonstration," *IEEE Trans. Ultrason., Ferroelect., Freq. Contr.*, vol. 39, no. 3, pp. 352–359, May 1992.

[22] ——, "Nonuniform phase distribution in ultrasound speckle analysis—Part II: Parametric expression and a frequency sweeping technique to measure mean scatterer spacing," *IEEE Trans. Ultrason., Ferroelect., Freq. Contr.*, vol. 39, no. 3, pp. 360–365, May 1992.

[23] A. Ohya, J. Kashioka, and M. Nakajima, "Relationship between regularity of scatterer's distribution and speckle appearing on ultrasonic echograms," in *Proc. 11th Symp. Ultrason. Elect., Kyoto 1990*, Kyoto, Japan, 1991.

[24] V. M. Narayanan, R. C. Molthen, P. M. Shankar, L. Vergara, and J. M. Reid, "Studies on ultrasonic scattering from quasi-periodic structures," *IEEE Trans. Ultrason., Ferroelect., Freq. Contr.*, vol. 44, no. 1, pp. 114–124, Jan. 1997.

[25] P. M. Shankar, R. Molthen, V. M. Narayanan, J. M. Reid, V. Genis, F. Forsberg, C. Piccoli, A. E. Lindenmayer, and B. B. Goldberg, "Studies on the use of non-Rayleigh statistics for ultrasonic tissue characterization," *Ultrason. Med. Biol.*, vol. 22, no. 7, pp. 873–882, 1996.

[26] U. R. Abeyratne, A. P. Petropulu, and J. M. Reid, "On modeling the tissue response from ultrasonic B-scan images," *IEEE Trans. Med. Imag.*, vol. 15, no. 4, pp. 479–490, Aug. 1996.

[27] D. R. Cox and P.A.W. Lewis, *The Statistical Analysis of Series of Events*. New York, NY: Wiley, 1966.

[28] D. Phillips, R. Cramblitt, and K. J. Parker, "Evaluation of a three dimensional fractal model of ultrasound scattering in liver," in *22nd Int. Symp. Ultrason. Imag. Tissue Characterization*, Arlington, VA, June 1997.

Robert M. Cramblitt (S'92–M'93) received the B.S. and M.S. degrees in electrical engineering from the University of Delaware in 1981 and 1983, respectively. He joined the Remote Sensing Group of the Johns Hopkins Applied Physics Laboratory in 1983, where he developed and analyzed low-light-level imaging systems for ocean measurement programs until 1989. He became a U.S. Air Force Laboratory Graduate Fellow at Purdue University and completed his doctoral degree in electrical engineering in 1994. He was a visiting professor at Purdue before joining the Center for Electronic Imaging Systems at the University of Rochester as a postdoctoral Research Associate in 1995. While there he developed image compression algorithms and speckle statistics models for the Rochester Center for Biomedical Ultrasound. He joined SVS, Inc., Albuquerque, NM, in 1997 where he has developed imaging alorithms for 3-D measurement, tracking and system simulations.

His research interests include image analysis and the modeling of imaging systems, with an amphasis on developing new methods to extract and use information to improve remote sensing and biomedical measurements.

Kevin J. Parker (S'79–M'81–SM'87–F'95) received the BS degree in engineering science, summa cum laude, from SUNY at Buffalo in 1976. Graduate work in electrical engineering was done at MIT, with MS and PhD degrees received in 1978 and 1981. From 1981 to 1985 he was an assistant professor of electrical engineering and radiology. Dr. Parker has received awards from the National Institute of General Medical Sciences (1979), the Lilly Teaching Endowment (1982), the IBM Supercomputing Competition (1989), the World Federation of Ultrasound in Medicine and Biology (1991). He is a member of the IEEE Sonics and Ultrasonics Symposium Technical Committee and serves as reviewer and consultant for a number of journals and institutions. He is also a member of the IEEE, the Acoustical Society of America, and the American Institute of Ultrasound in Medicine. He has been named a fellow in both the IEEE and the AIUM for his work in medical imaging. Dr. Parker's research interests are in medical imaging, linear and nonlinear acoustics, and digital halftoning.